

Research on fault diagnosis of indicator diagram based on BP neural network optimized by iterative learning control

Xiaohong Hao^{1, a}, Ning Zhang^{1, b}

¹School of Computer and Communication, Lanzhou University of Technology, Lanzhou, 730050, China.

^ahaoxhlut@163.com, *Corresponding author Email: ^byouruining@126.com

Keywords: pumping unit, fault diagnosis, indicator diagram, Shape invariant moment, Fourier descriptor, Iterative learning control, BP neural network.

Abstract: In this paper, an intelligent fault diagnosis method is presented to solve the problem that the accuracy of pumping unit fault diagnosis is not high. This method selects the Shape invariant moment and the Fourier descriptor to extract the characteristic parameters of the sample indicator diagram, and uses the BP neural network optimized by iterative learning control to classify and identify. Finally, the expert diagnosis method is used to compare the recognition results to obtain the diagnosis result. The experiment shows that the method is fast, accurate and intelligent.

1. Introduction

The oil resources have become the material basis of human survival and development, and play an extremely important strategic position in the national economy. Crude oil production process commonly used pumping unit, most pumping units work in unattended state, and the pumping unit underground condition is complex, and the load varies with the oiling process [1], which leads to the malfunction of the pumping unit is often affect the output and benefit of oil field.

After years of research and practice by scientific and technical workers at home and abroad, put forward some traditional methods such as: "five fingers dynamometer analysis"[2], the analysis method of the ground indicator diagram, the downhole indicator diagram diagnostic method, computer diagnosis method and so on. U.Tech.TexaS is the first application of artificial neural network to indicator diagram diagnosis [3], it can be used to identify the basic indicator diagram. In 1991, Siwei Zhang used fault tree analysis technology to establish an expert system for pumping pump diagnosis. Practice shows that the system is feasible [4]. In 1996, Zhijian Pan, Jiali Ge and others introduced the adaptive resonant network model, established a self-organizing neural network based on competitive learning, self-stabilization function model, 100 wells were measured on the ground, basic satisfactory identification results are obtained [5]. In 2004, Lijian Yang, Shiwen Xu and others studied the fault diagnosis of pumping unit based on BP neural network, and used the Gibbs wave equation to process the measured indicator diagram, and then extracted the characteristics of the indicator diagram as the training model of neural network. On the basis of predecessors, in this paper, a new fault diagnosis method is presented to solve the problem that the accuracy of pumping unit fault diagnosis is not high. This method selects the Shape invariant moment and the Fourier descriptor to extract the characteristic parameters of the sample indicator diagram, and uses the BP neural network optimized by iterative learning control to classify and identify. Finally, the expert diagnosis method is used to compare the recognition results to obtain the diagnosis result.

2. Indicator diagram

2.1 Indicator diagram meaning.

Indicator diagram refers to: in the process of pumping unit swabbing, polished rod ascent to the top, down to the most low-end, defined from the most low-end position as a starting point to pumping unit displacement of the polished rod with respect to the most low-end is taken as the horizontal axis,

and the load received by the rod is taken as the longitudinal axis. It can be drawn in a pumping process in the closed curve, namely the indicator diagram of pumping unit in the swabbing period [6]. Normal indicator diagram is shown in figure 1 below: the horizontal axis shows displacement (m), the vertical axis represents the load (kN).

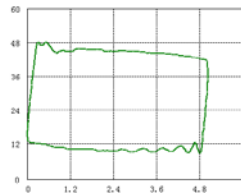


Fig. 1 Normal indicator diagram

2.2 Fault type analysis of indicator diagram.

All experimental datas of this paper are obtained from the oil and gas product IOT system (A11) of China National Petroleum Corporation. From the system, the 20 main faults of indicator diagram are studied: the inadequate supply of oil, oil thick, oil well sand production, the effect of gas, gas lock phenomenon, fixed valve leakage, traveling valve leakage, double valve leakage, travelling valve closed slowly, the plunger out of working barrel and pump, touch on the pump, pump rod under the touch, polished rod hit the donkey head, oil well paraffinication, sucker rod parting, travelling valve stuck normally open (plunger not into working barrel and pump), pumping with gushing, plunger stuck, the gap between plunger and pump cylinder is too large, liquid hammer and so on. These 20 kinds of fault indicator diagram will be used as teachers signal in BP neural network training.

3. A method for diagnosis of indicator diagram based on BP neural network optimized by iterative learning control Indicator diagram

The indicator diagram diagnosis method described in this article is basically divided into three stages: the first stage is the extraction of the characteristic parameters of the indicator diagram; the second stage is the classification and identification of the indicator diagram fault diagnosis; the third stage is to compare the recognition results and expert diagnosis, finally, the diagnosis results are obtained.

3.1 The extraction of the characteristic parameters of the indicator diagram.

In the process of working condition of pumping unit diagnosis, whether or not the indicator diagram characteristic parameters extracted can accurately characterize the characteristics of the graph curve has a decisive effect on diagnosis results [6]. In this paper, a new method combining shape invariant moments with Fourier descriptors is proposed to improve the speed and reduce the computational complexity. The new method has the advantages of stability of graph rotation, scale and translation invariance.

3.1.1 Indicator diagram pretreatment.

At present, indicator diagrams are closed curves real-time measured by the indicator instrument in the pumping unit. Each pumping unit updated an indicator diagram every half an hour. each indicator diagram is made up of 250 points. In order to facilitate feature extraction for training. We first need to preprocess the sample indicator diagrams, namely normalized processing, to ensure that the training time and the convergence speed of the network. I select max_min transformation normalized method.

$$X = \frac{i - i_{\min}}{i_{\max} - i_{\min}}$$

This article carries on the indicator diagram normalized processing based on formula:

$$Y = \frac{j - j_{\min}}{j_{\max} - j_{\min}}$$

, through the two basic formulas, the maximum value of the abscissa of the characteristic points of the indicator diagram is $i_{\max}=1$, the minimum value is $i_{\min}=0$; the maximum value of the ordinate is $j_{\max}=1$, the minimum value is $j_{\min}=0$. The sample indicator diagram can be normalized to 1 of the maximum horizontal and vertical coordinates by normalization of each point coordinate. For example, figure 2 shows the normalized graph of the touch on the pump:

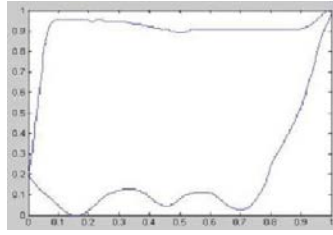


Fig. 2 The normalized graph of the touch on the pump

3.1.2 Shape invariant moment.

Invariant moment theory is first proposed by Minggui Hu, a Chinese-American, in 1961 [7]. Invariant moment has good invariance and antijamming ability for the graphs with translation, rotation and scale change, so it can reflect the essential characteristics of the graph effectively. Based on this, the invariant moment feature of the extracted power diagram can be regarded as its identified characteristic parameters.

For any nonnegative integer p, q , the $(p + q)$ order moment of the two-dimensional image $f(x, y)$ is:

$$m_{pq} = \sum_x \sum_y x^p y^q f(x, y),$$

where $f(x, y)$ is the grayscale of the image. Order $(p + q)$ center

distance is defined as:

$$\mu_{pq} = \sum_x \sum_y (x - x_0)^p (y - y_0)^q f(x, y), \quad x_0 = \frac{m_{10}}{m_{00}}, \quad y_0 = \frac{m_{01}}{m_{00}}$$

image M denotes the center of gravity of the image in the horizontal direction, and n denotes the center of gravity of the image in the vertical direction. The normalized $(p + q)$ order center distance is defined

as:

$$\eta_{pq} = \frac{\mu_{pq}}{\mu_{00}^r}, \quad \text{where } r = \frac{p+q}{2} + 1, \quad p+q=2, 3, 4, \dots$$

Then, 7 invariant moments can be obtained by normalization: $\varphi_1, \varphi_2, \varphi_3, \varphi_4, \varphi_5, \varphi_6, \varphi_7$:

$$\varphi_1 = \eta_{20} + \eta_{02} \tag{1}$$

$$\varphi_2 = (\eta_{20} - \eta_{32})^2 + 4\eta_{11}^2 \tag{2}$$

$$\varphi_3 = (\eta_{30} - 3\eta_{12})^2 + (3\eta_{21} - \eta_{03})^2 \tag{3}$$

$$\varphi_4 = (\eta_{30} + \eta_{12})^2 + (\eta_{21} + \eta_{03})^2 \tag{4}$$

$$\varphi_5 = (\eta_{30} - 3\eta_{12})(\eta_{30} + \eta_{12})[(\eta_{30} + \eta_{12})^2 - 3(\eta_{21} + \eta_{03})^2] + (3\eta_{21} + \eta_{03})(\eta_{21} + \eta_{03})[3(\eta_{30} + \eta_{12}) - (\eta_{21} + \eta_{03})^2] \tag{5}$$

$$\varphi_6 = (\eta_{20} - \eta_{02})[(\eta_{30} + \eta_{12})^2 - (\eta_{21} + \eta_{03})^2] + 4\eta_{11}(\eta_{30} + \eta_{12})(\eta_{21} + \eta_{03}) \tag{6}$$

$$\varphi_7 = (3\eta_{12} - \eta_{30})(\eta_{30} + \eta_{12})[(\eta_{30} + \eta_{12})^2 - 3(\eta_{21} + \eta_{03})^2] + 3(\eta_{21} - \eta_{03})(\eta_{21} + \eta_{03})[3(\eta_{30} + \eta_{12})^2 - (\eta_{21} + \eta_{03})^2] \tag{7}$$

According to the formula to calculate the above 20 kinds of fault indicator diagram and the normal indicator diagram moment vector with $\Phi = [\varphi_1, \varphi_2, \varphi_3, \varphi_4, \varphi_5, \varphi_6, \varphi_7]$ constitute classification statistical characteristic vectors are shown in table 1 below: The numbers 1 to 21 in the table correspond to the normal indicator diagram and the 20 types of fault indicator diagrams in the second title.

Table 1 Moment Eigenvector of 20 Faults and Normal indicator diagram

| Number | φ_1 | φ_2 | φ_3 | φ_4 | φ_5 | φ_6 | φ_7 |
|--------|-------------|-------------|-------------|-------------|-------------|-------------|-------------|
| 1 | 0.9681 | 1.6204 | 1.2028 | 0.5903 | 1.5013 | 0.2064 | 1.9008 |
| 2 | 0.8524 | 1.5834 | 1.3905 | 0.6219 | 1.4998 | 1.2937 | 1.4006 |
| 3 | 0.9587 | 1.6307 | 1.3948 | 0.0512 | 0.3298 | 0.6012 | 0.5832 |
| 4 | 0.8824 | 1.5729 | 1.3802 | 0.5813 | 1.4825 | 1.2876 | 1.3998 |
| 5 | 1.0398 | 1.9307 | 1.7094 | 0.0736 | 0.6887 | 0.6569 | 0.4023 |
| 6 | 0.9945 | 1.6706 | 0.8402 | 0.7808 | 1.6739 | 1.5604 | 0.7735 |
| 7 | 0.9588 | 1.5313 | 1.2847 | 0.0063 | 0.3856 | 0.5915 | 0.3826 |
| 8 | 1.0276 | 1.9035 | 0.7124 | 0.1389 | 0.3971 | 1.5903 | 0.1154 |
| 9 | 1.0117 | 1.8943 | 0.6875 | 0.1286 | 0.3835 | 1.5107 | 0.1271 |
| 10 | 0.9924 | 1.8235 | 0.6933 | 0.1267 | 0.3924 | 1.5269 | 0.1275 |
| 11 | 0.9671 | 1.5835 | 1.2845 | 0.0356 | 0.3216 | 0.5987 | 0.4935 |
| 12 | 0.9825 | 1.6614 | 1.1978 | 0.7835 | 1.2497 | 0.2464 | 1.2451 |
| 13 | 0.9608 | 1.6839 | 1.6398 | 0.0521 | 0.3721 | 0.6138 | 0.5832 |
| 14 | 0.9565 | 1.7034 | 1.4065 | 0.0497 | 0.3443 | 0.5962 | 0.5781 |
| 15 | 0.9501 | 1.7046 | 1.3967 | 0.0502 | 0.4109 | 0.6002 | 0.5298 |
| 16 | 0.9945 | 1.9706 | 0.9402 | 0.9206 | 1.8154 | 1.8904 | 0.6538 |
| 17 | 0.9928 | 1.8747 | 0.9208 | 0.8946 | 1.7935 | 1.7936 | 0.6829 |
| 18 | 0.9957 | 1.9699 | 0.9309 | 0.9111 | 1.8032 | 1.8847 | 0.6324 |
| 19 | 0.9085 | 0.0246 | 0.0079 | 0.0335 | 0.0483 | 0.0052 | 0.2032 |
| 20 | 0.8066 | 1.2046 | 0.6508 | 0.0355 | 0.5893 | 0.5801 | 0.0003 |
| 21 | 0.9835 | 1.4235 | 1.3203 | 0.0325 | 0.4411 | 0.4902 | 0.0002 |

3.1.3 Fourier descriptor.

The Fourier descriptor Extraction is to do the Fourier transform of the object coordinate sequence, The exact shape of the object, only need to intercept the approximate shape of the low-frequency coefficient, it can be used as a basis for judging the pattern recognition [8].

In this paper, the complex coordinate function is used to describe the curve. Take a closed, continuous, smooth curve on the xoy plane, taking any point on the curve as the starting point (x0 , y0), N points are taken in clockwise direction to (xN , yN). we can obtain a coordinate sequence x, y representing the boundary of the curve. The N +1 horizontal and vertical coordinates assigned to U: $U(n) = x(n) + jy(n)$, where n = 0,1, ... N, U is a complex variable, the abscissa x is a real part and the ordinate y is an imaginary part. U(n)is a shape to the boundary as the function of cycle, do fast Fourier

$$a(k) = FFT[U(n)] = \sum_{n=0}^N U(n)e^{-j\frac{2\pi nk}{N}}$$

transform: , Among them, k = 0,1, ... N, Fourier coefficient a (k) is to describe the shape of the boundary curve Fourier descriptor. These Fourier descriptors can recover

$$U(n) = IFFT[a(k)] = \frac{1}{N+1} \sum_{k=0}^N a(k)e^{j\frac{2\pi nk}{N}}$$

U(n) by inverse Fourier transform, namely , Among them, n = 0, 1,... N, if only use first P Fourier descriptors in the low frequency area. Even if a (k) = 0, k> P-1

$$\hat{U}(n) = IFFT[a(k)] = \frac{1}{N+1} \sum_{k=0}^{P-1} a(k)e^{j\frac{2\pi nk}{N}}$$

in the preceding equation, it can be rewritten as: , Where n = 0, 1, ..., N. Through a large amount of data tests, we can select Fourier descriptor P=10 to identify indicator diagram outline. Because the Fourier descriptor will be affected by the location of the curve vertices, the shape of the curve direction and the proportion of changes. In order to eliminate these effects, we need to normalize them.

3.1.4 Feature extraction of indicator diagram based on shape invariant moment and Fourier descriptor.

Although the shape invariant moment method is robust and its algorithm is simple, its computational complexity increases with the increase of order, and the computational complexity is still large, which is not suitable for real-time applications. The Fourier descriptor algorithm is simple,

the amount of computation is small, suitable for real-time applications, but vulnerable to noise interference, lack of stability, so we can consider the combination of the two methods: Firstly, the moment feature sequence is obtained to express the shape of the indicator diagram. then the Fourier transform of the sequence is normalized again. Eventually we can get the feature descriptor with translation, rotation and scale invariant, namely the characteristic parameters of indicator diagram. The torque characteristic vectors table 1 are Fourier transformed and Gaussian normalized as shown in table 2 below:

Table 2 Moment Eigenvector Fourier Descriptors of 20 Faults and Normal indicator diagram

| Number | C ₁ | C ₂ | C ₃ | C ₄ | C ₅ | C ₆ | C ₇ |
|--------|----------------|----------------|----------------|----------------|----------------|----------------|----------------|
| 1 | 0.5312 | 0.3732 | 0.4325 | 0.8796 | 0.4325 | 0.3732 | 0.5312 |
| 2 | 0.4503 | 0.4625 | 0.4019 | 0.8973 | 0.4019 | 0.4625 | 0.4503 |
| 3 | 0.3324 | 0.4032 | 0.5141 | 0.8806 | 0.5141 | 0.4032 | 0.3324 |
| 4 | 0.3522 | 0.4407 | 0.5033 | 0.8947 | 0.5033 | 0.4407 | 0.3522 |
| 5 | 0.3624 | 0.4589 | 0.5136 | 0.9004 | 0.5136 | 0.4589 | 0.3624 |
| 6 | 0.3917 | 0.4826 | 0.3889 | 0.8731 | 0.3889 | 0.4826 | 0.3917 |
| 7 | 0.3408 | 0.4127 | 0.5314 | 0.8745 | 0.5314 | 0.4127 | 0.3408 |
| 8 | 0.3925 | 0.5338 | 0.4105 | 0.8839 | 0.4105 | 0.5338 | 0.3925 |
| 9 | 0.3814 | 0.4994 | 0.4096 | 0.8715 | 0.4096 | 0.4994 | 0.3814 |
| 10 | 0.3645 | 0.4746 | 0.5336 | 0.9024 | 0.5336 | 0.4746 | 0.3645 |
| 11 | 0.3913 | 0.5287 | 0.4087 | 0.8902 | 0.4087 | 0.5287 | 0.3913 |
| 12 | 0.3536 | 0.4543 | 0.5156 | 0.8983 | 0.5156 | 0.4543 | 0.3536 |
| 13 | 0.3467 | 0.4513 | 0.5102 | 0.8913 | 0.5102 | 0.4513 | 0.3467 |
| 14 | 0.3503 | 0.4581 | 0.5321 | 0.8756 | 0.5321 | 0.4581 | 0.3503 |
| 15 | 0.3482 | 0.4427 | 0.5046 | 0.8942 | 0.5046 | 0.4427 | 0.3482 |
| 16 | 0.4004 | 0.5178 | 0.4039 | 0.9016 | 0.4039 | 0.5178 | 0.4004 |
| 17 | 0.3954 | 0.5088 | 0.4006 | 0.8907 | 0.4006 | 0.5088 | 0.3954 |
| 18 | 0.3897 | 0.4996 | 0.3924 | 0.8889 | 0.3924 | 0.4996 | 0.3897 |
| 19 | 0.3416 | 0.3682 | 0.3314 | 0.8902 | 0.3314 | 0.3682 | 0.3416 |
| 20 | 0.3411 | 0.4481 | 0.5257 | 0.8704 | 0.5257 | 0.4481 | 0.3411 |
| 21 | 0.3392 | 0.4328 | 0.5007 | 0.8689 | 0.5007 | 0.4328 | 0.3392 |

3.2 Fault classification and identification of indicator diagram based on BP neural network optimized by iterative learning control.

The BP neural network is proposed by Rumelhart and Mc Celland [9] led the research team in 1986. It has simple structure, strong plasticity. It consists of three layers [10], including the input layer, the hidden layer, the output layer, the network adjacent layer neurons are connected, called the network connection weights.

$$u_i^l = f\left(\sum_{n=1}^N \eta_{ni} x_{kn}\right) \tag{8}$$

The output of each layer neuron of BP neural network is:

Where η_{ni} represents the connection weights of the nth node and the ith node of the adjacent layer, x_{kn} represents the input sample, u_i^l represents the output of the ith node of the layer I, $f(\cdot)$

represents the activation function, usually using nonlinear sigmoid function, i.e., $f(x) = \frac{1}{1+e^{-x}}$, it can convert the input to the output between [0, 1], the nonlinear mapping of input and output is realized by adjusting the magnification factor. The output error of the j neuron in the output layer is:

$$e_{kj} = v_{kj} - y_{kj} \tag{9}$$

where v_{kj} represents the expected output of the jth neuron; y_{kj} is the actual output of the jth neuron during the first j learning training.

$$E^N(k) = \frac{1}{2} \sum_{j=1}^J e_{kj}^2$$

After inputting the Nth sample, the error sum of all nodes in the output layer is:
(10)

$$\omega_{ij}^N(k+1) = \omega_{ij}^N(k) + \mu \frac{\partial E^N(k)}{\partial \omega_{ij}^N(k)}$$

Network weight correction algorithm is:

$$\mu \frac{\partial E^N(k)}{\partial \omega_{ij}^N(k)}$$

where k is the number of training, $\mu \frac{\partial E^N(k)}{\partial \omega_{ij}^N(k)}$ represents the gradient of the error to the weight, and μ represents the learning step.

Because BP neural network has some disadvantages such as slow convergence rate and local minima in the training process, it needs to be optimized. In this paper, the iterative learning control is used to optimize the neural network. The BP neural network based on optimization theory is excellent in the convergence speed and the improvement of the local minimum.

At present, the more effective weight correction method is to increase the momentum term, the formula is: $\omega_{ij}(k+1) = \omega_{ij}(k) + \Delta\omega_{ij}(k)$ (12)

$$\Delta\omega_{ij}(k) = \alpha\Delta\omega_{ij}(k-1) + \mu \frac{\partial E}{\partial \omega_{ij}(k)}$$

where α is the momentum factor, $\alpha \in (0,1)$ is generally used. Formula (12) and (13) consider the error gradient descent direction before k and k at the same time. the training process reduces the vibration and accelerates the convergence. It is an improvement on the basis of the error sum of all nodes in the output layer.

Iterative learning control is to use the previous system input information and tracking error to modify the current control input, through a certain number of repetitions to achieve the output can be completely or asymptotically tracking the desired trajectory. Therefore, we can consider the idea of iterative learning control to improve the conventional training algorithm of BP neural network. In this

paper, we will use iterative study of D control algorithm learning rate [11]: $u_{k+1}(t) = u_k(t) + \Gamma_d \frac{de_k(t)}{dt}$, where k is the number of iterations and Γ is the constant gain. The weights of BP neural network are modified by (12) to optimize the BP algorithm to avoid the problem of slow convergence and local minima. A new iterative learning neural network weight training algorithm is proposed. Considering the sum of the output errors of the two training samples, and using the output error of the previous training process to correct the weights. We use the differential of output error on weight value to modify the weight value. And recycling of adjacent two training output error to fix network weights, namely according to the idea of iterative learning control, the error of the previous sample set N-1 is differential to modify the network weights, the formula is:

$\omega_{ij}^N(k+1) = \omega_{ij}^N(k) + \mu \frac{\partial E^N(k)}{\partial \omega_{ij}^N(k)} + \lambda \frac{\partial E^{N-1}(k)}{\partial \omega_{ij}^{N-1}(k)}$, where N is the sample set, N-1 is the previous training sample set, K is the training number of the network, and λ is the training learning gain.

BP neural network optimized by iterative learning control: Firstly, 7 eigenvalues extracted by 3.1 feature map are used as the input vectors of BP neural network, and the number of nodes in input layer, hidden layer and output layer are selected rationally. Input the sample set, and according to the formula (8) to calculate the output of the hidden layer and output layer nodes, then according to the formula (9) and (10) to calculate the output error of each layer nodes, and then modify the network weight according to formula (13). Secondly, we set an acceptable minimum error ε , and then use formula (10) to calculate the mean square error E of the training network. Compare the size of E and ε . If $E < \varepsilon$, the network training is finished. If $E > \varepsilon$, then it enters a new round of training and learning, and after several iterations, it reaches to $E < \varepsilon$ before iteration training is finished. And get the desired output value, that is, the better indicator diagram fault classification results.

3.3 Expert diagnostic method.

Combined with oil field data, by searching the historical data of the known diagnosis results, we find out some common characteristics of these data items, For each fault type, find out the common problems of the relevant data and parameters of the pumping unit, such as moving liquid surface, output and load, summed up the diagnostic parameters and methods, established the diagnostic model, as shown in Table 3. According to the relevant data of the pumping unit for expert diagnosis, then compare the diagnostic results with the recognition results obtained by the above method. If the diagnostic results are consistent, the fault type can be determined. If the test results are not uniform, the recognition judgment needs to be repeated.

Table 3 Nine kinds of fault diagnosis model of expert algorithm library

| Diagnostic result | Expert diagnostic parameters and methods |
|------------------------------|--|
| The inadequate supply of oil | Moving surface close to the pump hanging depth or the distance between the two closer, less submerged |
| oil thick | $(\text{Maximum load} - \text{minimum load}) > \text{theoretical maximum load} * 0.6$ |
| the effect of gas | The current gas-liquid ratio is greater than the average gas-liquid ratio of more than 10% |
| gas lock phenomenon | Gas liquid ratio is greater than the average oil field gas liquid ratio above 100%, producing fluid volume = 0. |
| valve leakage | ① Production decreased; ② Moving liquid surface rise |
| oil well paraffinication | ① $(\text{maximum load} - \text{minimum load}) > \text{theoretical maximum load} - \text{theoretical minimum load}$; ② production > 0 |
| sucker rod parting | ① production = 0; ② $(\text{maximum load} - \text{minimum load}) < (\text{maximum load} - \text{theoretical minimum load}) * 0.4$ |
| pumping with gushing | ① current production > theoretical yield; ② liquid < 100m, the surface in the wellhead |
| plunger stuck | ① power balance degree > 1.5; ② production = 0; ③ moving liquid surface rise |

4. The simulation and verification of indicator diagram diagnosis

Based on the above 20 kinds of demonstration models, In this paper, I select 100 kinds of fault cases and 100 normal work plans from the oil and gas product IOT system (A11) project database of China National Petroleum Corporation. A total of 2100 samples of the indicator diagram as the simulation of the training sample set. Among them, 60 indicator diagrams of each fault type were selected, that is, the number of training times was 1260, error precision is 0.0012, and the remaining 40 graphs are used as test samples, that is, a total of 840 indicator diagrams as a simulation of test sample set. According to the above-mentioned method, we can carry on the fault diagnosis simulation of the sample indicator diagram.

In the process of model training in MATLAB, the 7 eigenvalues extracted from the corresponding nodes of the input layer are simulated. The type of recognition is the work type in the field data, so the output node corresponds to the 21 working states to be identified, that is, the number of output node is 21, and the number of the hidden layer node is 12 constructed by empirical method and experiment, forming a 7-12-21 network. The time of feature extraction is 78.2s, and the training time of iterative learning BP neural network is 2.6s. After the training, the test sample model was used to test, the recognition error was 5.64%, After the training, the test sample model is used to test, and the recognition error was 5.83%. And the average time needed for the model to recognize a indicator diagram was 2.8ms. The test results show that the model has high accuracy and recognition speed for recognition and classification of indicator diagram, and it can meet the requirements of real-time and accurate diagnosis of indicator diagram fault.

In order to verify this method has better performance compared to traditional methods, under the same test sample set, Reference [12] uses the traditional BP neural network classifier, reference [13] uses SVM classifier to test the sample, and compared with the BP neural network diagnosis method optimized by iterative learning control, we can get results as shown in table 4: The numbers 1 to 3 in the table correspond to the traditional BP neural network, SVM, the BP neural network optimized by iterative learning control.

Table 4 Comparison of diagnostic methods

| Number | Number of samples | Correct number | identification time/ms | Correct recognition rate/% |
|--------|-------------------|----------------|------------------------|----------------------------|
| 1 | 840 | 698 | 1.9 | 83.09 |
| 2 | 840 | 671 | 11.6 | 79.88 |
| 3 | 840 | 791 | 2.8 | 94.17 |

The result shows SVM classifier shows good recognition effect when the sample size is small. The number of real-time indicator diagram data is very large, so it can not be recognized accurately by SVM classifier.

5. Conclusions

From the test process and the results, it is shown that the performance of the diagnostic method proposed in this paper has certain advantages: The recognition time is improved by about 9 ms relative to the support vector machine identification method. In the same test sample cases, the accuracy of the diagnosis increased from 83.09% and 79.88% to 94.17%. So the intelligent fault diagnosis method presented in this paper is more suitable for real-time fault diagnosis of large on-site indicator diagram data in oil field. It not only makes up for the lack of existing diagnostic methods. But also has good comprehensive performance, and it can shorten the training time, improve the training speed, and has the ability of high accuracy of recognition accuracy. But different models of the indicator instrument can be used in different fields, their performance is also different, so in the follow-up work, I will further optimize the diagnosis algorithm to improve the versatility and robustness of the algorithm. and combined with the oil field practice, rich expert algorithms library, so that I can further enhance the diagnostic accuracy of the algorithm.

References

- [1] Hongbing Xie, Qiulin Guo, Feng Li. Prediction of petroleum exploration risk and subterranean spatial distribution of hydrocarbon accumulations[J]. *Petroleum Science*,2011,8(1):17-23.
- [2] Yechen Tian. Application of neural network based on cuckoo search algorithm in pumping fault diagnosis [D]. Northeast Petroleum University, 2016.
- [3] Bilong WEN, Zhiquan WANG, Zongze JIN, Man XU, Zhan Shi. Fault Diagnosis of Pumping Unit Combined with Demonstration and Fuzzy Neural Network [J]. *Journal of Computer Applications*, 2016 (01): 121-125.
- [4] Xin Chen. Research on the inversion and identification of indicator diagram based on neural network [D]. Beijing Institute of Technology, 2015.
- [5] Xinqi Zhou. Research on pumping unit fault diagnosis based on the fish network neural network[D]. Northeast Petroleum University, 2015.
- [6] Xiaohan Wang. Research on the method of feature extraction for indicator diagram fault diagnosis system [D]. Qingdao: China University of Petroleum, 2011.
- [7] Yang Yu, Jiabin Liang, Mengge Li. Image Feature Extraction of Standardized HU Invariant Moment Algorithm [J]. *Journal of Shenyang University of Technology*, 2016 (06): 72-76

- [8] Zhengchu Peng. Research on Shape Recognition based on Fourier Descriptor [D]. Harbin Institute of Technology, 2016.
- [9] Rumelhart D E, Hinton G E, Williams R J. Learning representations by back-propagating errors[J]. Cognitive modeling, 1988.
- [10]Luqi, Jiang. Wensheng Sun. Network traffic prediction model based on improved BP neural network [J]. Communication Technology, 2017, (01): 68-73.
- [11]Xiaoyong Zhou, Chunyan Zhai, Shuchen Li, Chengli Su. BP neural network weights training algorithm based on Iterative learning [J]. Journal of Liaoning Shihua University, 2013, (04): 83-86.
- [12]Zhuo Liu, et al. Research on pump power diagnosis method based on BP neural network and moment invariant features [J]. Manufacturing Automation, 2013.
- [13]Chunsheng Li, et al. Study on identification of pumping unit work indicator diagram based on support vector machine [J]. Journal of Computer Technology and Development, 2014.